Phase transition in the vortex liquid and the critical endpoint in $YBa_2Cu_3O_y$

Kenji Shibata,[1] Terukazu Nishizaki,[1,2,*] Takahiko Sasaki,[1,2] and Norio Kobayashi[1,2,3]
[1]*Institute for Materials Research, Tohoku University, Sendai 980-8577, Japan*
[2]*CREST, Japan Science and Technology Corporation, Kawaguchi 332-0012, Japan*
[3]*Center for Low Temperature Science, Tohoku University, Sendai 980-8577, Japan*
(Received 15 April 2002; published 23 December 2002)

The vortex phase diagram of optimally doped untwinned $YBa_2Cu_3O_y$ is studied. We find a first-order transition $T_L(H)$ in the vortex liquid above the terminal point H_{mcp} ($\simeq 7$ T) of both the vortex glass line $T_g(H)$ and the field-driven disordering transition line $H^*(T)$. The obtained small entropy change (~ 0.02 k_B/vortex/layer) and the critical endpoint H_{cep} ($\simeq 11$ T) of the $T_L(H)$ line indicate that the vortex liquid undergoes the vortex slush regime before the solidification into the vortex glass phase. Below H_{mcp}, the vortex liquid phase shows the first-order melting transition into the Bragg glass phase. We also study the oxygen content y dependence of the vortex phase diagram and find that the vortex slush regime is located in the borderline (i.e., $6.90 \leqslant y \leqslant 6.92$) below which the vortex lattice melting transition disappears. The result indicates that the point disorder with the intermediate strength plays an important role in the vortex slush regime.

DOI: 10.1103/PhysRevB.66.214518 PACS number(s): 74.60.Ge, 74.25.Bt, 74.72.Bk

I. INTRODUCTION

In high-temperature superconductors, vortex matter shows pronounced features due to strong thermal fluctuations which result from the high critical temperature T_c, the short coherence length ξ, and the large anisotropy $\gamma=(m_c/m_{ab})^{1/2}$ (Ref. 1). In clean untwinned $YBa_2Cu_3O_y$ (YBCO), studies on resistivity,[2,3] magnetization,[4,5] and specific heat[6–8] have demonstrated that the vortex liquid phase and the Bragg glass phase are separated by the first-order vortex lattice melting transition line $H_m(T)$. Since the nature of the vortex matter is very sensitive to the effective disorder which is controlled both by the type and density of defects and by the magnetic fields, the vortex lattice melting transition gives way to the continuous glassy transition in high fields above the multicritical point H_{mcp}.[3,5,9–11] Recent experiments in overdoped YBCO (Refs. 9–11) and theories[12–15] have suggested that the field-driven disordering transition line $H^*(T)$ is connected with H_{mcp} and divides the vortex solid into the Bragg glass and the vortex glass phases.

The vortex state is determined by the competition between elastic, pinning, and thermal energies,[1] so the vortex matter shows a great variety of phases near H_{mcp} due to the point disorder such as the deficiency. Contrary to overdoped YBCO,[9–11] the $H^*(T)$ line approaches the first-order transition line well below the critical point for optimally doped and slightly underdoped YBCO.[16–18] In addition, two separate transitions, i.e., the remnant of vortex lattice melting transition and the vortex glass transition, have been suggested for defect-enhanced YBCO.[19–21] In this paper, we find thermodynamic evidence of the first-order transition in the vortex liquid regime and the appearance of the critical endpoint for optimally doped YBCO. We show that these complicated vortex phases[16–19] are well explained by considering a vortex slush regime above H_{mcp}. We also study the oxygen content y dependence of the vortex phase diagram and find that the effective disorder with intermediate strength results in the vortex slush regime.

II. EXPERIMENT

High quality YBCO single crystals were prepared by the self-flux method using a Y_2O_3 crucible.[9,10] A sample used in this study was a naturally untwinned single crystal with dimensions of $1.55\times 0.80\times 0.02$ mm^3. The optimally doped crystal ($y\simeq 6.92$) prepared by annealing at 550 °C in 8 bar oxygen[16] showed $T_c=93.3$ K with the width ΔT_c (10% $-$ 90%) ~ 140 mK. The oxygen content y was estimated from the annealing condition and the T_c value.[16,22] Electric resistivity ρ was measured by a conventional dc four-probe method under a current density $J\simeq 0.1-10$ A/cm^2. High-precision magnetization measurements were performed using a capacitance torque meter in the magnetic field applied about $<10°$ tilted away from the c axis.[23] A sensitivity of the torque magnetometer was better than $\Delta\tau=1\times 10^{-11}$ Nm and the magnetization $M(H)$ was derived from a magnetic torque $\boldsymbol{\tau}=V(\boldsymbol{M}\times\mu_0\boldsymbol{H})$ curve.

III. RESULTS AND DISCUSSION

A. Anomalous transition in the resistivity

Figure 1 shows magnetic-field dependence of the linear resistivity $\rho(H)$ at several temperatures (72 K$\leqslant T\leqslant$90 K).

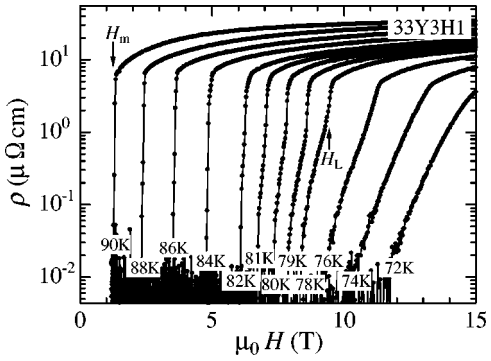

FIG. 1. Magnetic-field dependence of the linear resistivity ρ in optimally doped untwinned YBCO.

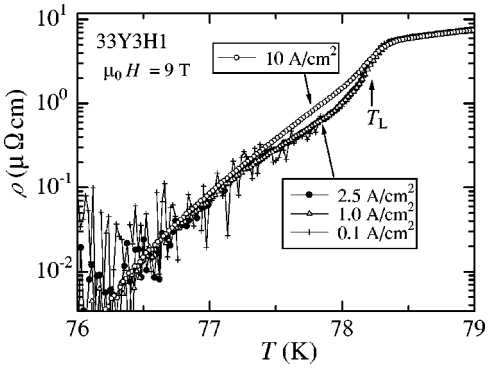

FIG. 2. Temperature dependence of the resistivity ρ at 9 T under various current densities J.

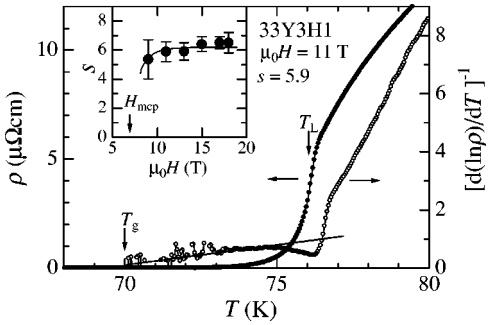

FIG. 3. Temperature dependence of ρ and $(d\ln\rho/dT)^{-1}$ at 11 T. Inset: Magnetic-field dependence of the critical exponent s above the multicritical point H_{mcp}.

In the high-temperature region above 81 K, $\rho(H)$ shows a sharp discontinuous jump at $H_{\mathrm{m}}(T)$ which is associated with the first-order vortex lattice melting transition.[2,3] On the other hand, in the low-temperature region below 74 K, a continuous decrease of $\rho(H)$ is observed, indicating the second-order transition such as the vortex glass transition.[24] In the intermediate-temperature region (76 K$\leqslant T\leqslant$81 K), $\rho(H)$ shows an anomalous two-step feature. Although $\rho(H)$ shows a sharp drop at H_{L}, a finite value of $\rho(H)$ remains and $\rho(H)$ decreases gradually with decreasing field. These results indicate that the vortex liquid undergoes two kinds of transition into the vortex solid, i.e., the first-order transition at H_{L} in the high-field region and the second-order transition in the low-field region.

Figure 2 shows temperature dependence of resistivity in the two-step region ($\mu_0 H=9$ T) under various transport current densities $J=0.1-10$ A/cm^2. The resistivity $\rho(T)$ in the lower current density ($J\leqslant 2.5$ A/cm^2) shows linear response (i.e., linear resistivity) in the whole temperature region studied and shows the sharp decrease at $T_{\mathrm{L}}(H)$, while $\rho(T)$ in the high current density ($J\geqslant 10$ A/cm^2) deviates upward from that in the lower current density. With decreasing temperature $\rho(T)$ gradually decreases in the same manner of $\rho(H)$ as shown in Fig. 1. In the lower-resistivity region, $\rho(T)$ shows linear response even in the high current density of 10 A/cm^2. Since the two-step feature is clear in the low current limit and the resistive tail shows the linear response, the two-step transition does not result from broadening by the depinning process which should be observed under high J above the critical current density in the vortex solid phase. Therefore, the gradual disappearance of the linear resistivity is consistent with the second-order solidification from the vortex liquid to the glass phase. The interesting nonlinearity of ρ in high J is a characteristic feature of the vortex state just below T_{L}. The origin of the nonlinearity is discussed below.

In order to examine the nature of the transition in the lower ρ region, the temperature dependence of ρ and $[\mathrm{d}(\ln\rho)/\mathrm{d}T]^{-1}$ at 11 T is shown in Fig. 3. Since the vortex glass theory[24] predicts the temperature dependence of the linear resistivity $\rho\propto(T-T_{\mathrm{g}})^{s}$, the vortex glass transition temperature T_{g} and the critical exponent s are derived from the linear extrapolation to $[\mathrm{d}(\ln\rho)/\mathrm{d}T]^{-1}=0$ and the inverse of the slope in $[\mathrm{d}(\ln\rho)/\mathrm{d}T]^{-1}$ versus T, respectively. As shown in the figure, $[\mathrm{d}(\ln\rho)/\mathrm{d}T]^{-1}$ has a dip structure near the resistive kink T_{L} and shows the linear relation when the temperature approaches T_{g}. The obtained value of the critical exponent $s=5.9$ is field independent in high fields well above the multicritical point H_{mcp} as shown in the inset of Fig. 3 and agrees with the previously reported results for untwinned YBCO.[3,10,25] This result indicates that the gradual transition near $T_{\mathrm{g}}(H)$ is described by the vortex glass theory.[24]

B. Thermodynamic properties of the vortex phase transition

Figure 4(a) shows a magnetization $M(H)$ curve at 85 K. The magnetization shows an anomalous feature at H_{m} which

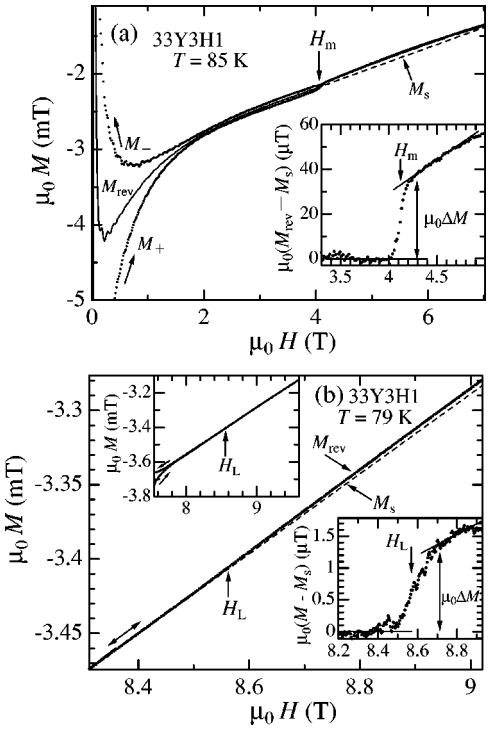

FIG. 4. (a) Magnetic-field dependence of the magnetization M at 85 K. Inset: Magnetization jump at H_{m}. (b) Magnetic-field dependence of M (upper inset) and expanded view of M (main panel) at 79 K. Lower inset: Magnetization jump at H_{L}.

separates irreversible and reversible regions. As shown in the inset of Fig. 4(a), a clear jump in the magnetization $\mu_0(M_{rev}-M_s)$ is observed at $\mu_0 H_m \simeq 4.1$ T and the jump height $\mu_0 \Delta M \simeq 34\ \mu$T shows a reasonable value for the first-order vortex lattice melting transition.[4,6,7,9] Here, M_{rev} is an equilibrium magnetization determined as an average of magnetization M_+ and M_- on the ascending and descending branches, respectively, and M_s is a linear extrapolation from the low-field magnetization. The first-order vortex lattice melting transition line $H_m(T)$ is observed above 81 K (i.e., below 7 T) and well agrees with the field at which ρ suddenly goes to zero without two-step feature. The small but finite vortex pinning below $H_m(T)$ is consistent with the topologically ordered Bragg glass phase.[12–15]

In the region of 76 K$\leqslant T \leqslant$81 K, on the other hand, the behavior of the phase transition is different from that discussed above. Figure 4(b) and the upper inset of Fig. 4(b) show the $M(H)$ curve at 79 K, and a tiny anomaly is observed at H_L. As shown in the lower inset of Fig. 4(b), a jump height in $M(H)$ is estimated to be $\mu_0 \Delta M \simeq 1.3\ \mu$T. The field $H_L(T)$ agrees well with the field at the resistive kink. Although the jump in both $M(H)$ and $\rho(H)$ implies the first-order transition, the jump is observed in the reversible magnetization region above $H_g(T)$ and ρ remains a finite value at $H_L(T)$. Furthermore, the jump height $\mu_0 \Delta M$ at $H_L(T)$ is an order-of-magnitude smaller than that for the vortex lattice melting transition. These results show that the transition at $H_L(T)$ is not consistent with the vortex lattice melting transition, implying a new type of transition in the vortex liquid. The two-step transition cannot be explained by means of the macroscopic inhomogeneity of the superconductivity, because the superconducting transition at zero field and the thermodynamic transitions at $H_m(T)$ and $H_L(T)$ are very sharp.

Below 75 K, $M(H)$ shows a steep increase at a characteristic magnetic field H^* below the second peak as reported previously.[9,10] The field H^*, which is defined by a sharp peak in dM/dH,[10] is interpreted as the field-driven disordering transition field between the Bragg glass phase and the vortex glass phase.[9–15] The disordering transition line $H^*(T)$ shifts to the high-field region with increasing temperature and finally reaches $\sim$7 T at $\sim$81 K.[17]

Figure 5 shows the vortex phase diagram for optimally doped YBCO. The relation between three transition lines of $T_m(H)$, $T_g(H)$, and $H^*(T)$, which meet at the multicritical point $\mu_0 H_{mcp} \simeq 7$ T, is consistent with the previously discussed phase diagram.[9–11] In the phase diagram, the vortex liquid phase undergoes the melting lines $T_g(H)$ and $T_m(H)$ into the vortex glass phase and the Bragg glass phase above and below H_{mcp}, respectively, and these two vortex solid phases are separated by $H^*(T)$. In Fig. 5, however, the existence of the $T_L(H)$ line and the critical endpoint of $T_L(H)$ makes the vortex phase diagram peculiar, because the $T_L(H)$ line implies the phase transition between the different vortex liquid regimes. The $T_L(H)$ line is smoothly connected with the $H_m(T)$ line and both lines are described by the same expression[2] for the first-order vortex lattice melting transition $H_m = H_0(1-T/T_c)^n$ with the reasonable parameters $\mu_0 H_0$

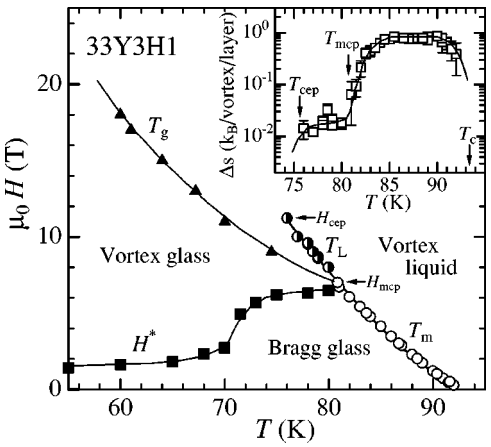

FIG. 5. Vortex phase diagram for optimally doped untwinned YBCO. Inset: Entropy change Δs at the first-order transition lines $T_m(H)$ and $T_L(H)$ as a function of temperature.

$=113.6$ T, $T_c = 93.3$ K, and $n = 1.38$, so the origin of the $T_L(H)$ can be greatly influenced by the vortex lattice melting transition.

The inset of Fig. 5 shows the temperature dependence of the entropy change Δs at the first-order transition which is determined by using the Clausius-Clapeyron equation $\Delta s = -d\phi_0(\Delta M/H_m)(dH_m/dT)$. Here, ϕ_0 is the flux quantum and $d \simeq 12$ Å is the distance between CuO_2 double layers. In the high-temperature region above 85 K, Δs due to the vortex lattice melting transition is almost temperature independent around $\sim 0.76 k_B$/vortex/CuO_2 double layer; the value of Δs well agrees with the previously reported value of 0.4–$0.8 k_B$/vortex/CuO_2 double layer.[4,6,7,9] Below 84 K, however, Δs drastically decreases with decreasing temperature toward the multicritical point $T_{mcp} \simeq 81$ K. In the region of 76 K$<T<$81 K, Δs on $T_L(H)$ shows weak temperature dependence with a tiny value ($\sim 0.02 k_B$/vortex/CuO_2 double layer) and disappears below the critical endpoint T_{cep} ($\simeq$76 K) of the $T_L(H)$ line. These results indicate that the terminal point of both $T_g(H)$ and $H^*(T)$ lines divides the first-order transition line into different two regions which consist of the vortex lattice melting transition line $T_m(H)$ and a novel transition line $T_L(H)$.

Since the first-order transition line $T_L(H)$ has a critical endpoint $\mu_0 H_{cep} \simeq 11$ T, one can enter the region between $T_g(H)$ and $T_L(H)$ continuously from the vortex liquid regime above $T_L(H)$ without a phase transition by going above the critical endpoint. The result indicates that there is no symmetry difference above and below the $T_L(H)$ line similar to the case of liquid-gas transition of water. Furthermore, $\rho(T)$ shows a much smaller but finite value below $T_L(H)$ as shown in Figs. 1 and 2. Thus the vortex state in the region between $T_g(H)$ and $T_L(H)$ is considered as the pinned vortex liquid. Vinokur *et al.*[26] have discussed the pinning effect on the vortex liquid by the weak disorder. They have suggested that the vortex liquid can be effectively pinned and the energy barrier U_{pl} for the plastic deformation of vortices becomes larger when a characteristic time of the plastic deformation of vortices τ_{pl} is larger than that of the pinning τ_{pin}.[1,26] The thermally assisted flux flow (TAFF) with a re-

sistivity $\rho=\rho_0\exp(-U_{\rm pl}/k_{\rm B}T)$ is expected in the pinned liquid regime and the crossover to the unpinned vortex liquid takes place with increasing temperature. Although a broad shoulder in $\rho(T)$ has been interpreted as the crossover from the pinned liquid with a large viscosity to the unpinned liquid with a flux flow resistivity,[26] it is difficult to explain the sharp phase transition at $T_{\rm L}(H)$ by this model.

The phase transition in the vortex liquid and the concept of the vortex slush as a possible explanation of the pinned liquid regime between $T_{\rm g}(H)$ and $T_{\rm L}(H)$ have been proposed by Worthington *et al.*[19] and theoretically discussed by Ikeda.[27] Across $T_{\rm L}(H)$ into the vortex slush regime, vortices have short-range translational order but no long-range phase order, so the energy barrier of the vortex motion does not diverge and $\rho(T)$ shows a finite value in the low-J limit. However, $\rho(T)$ in the vortex slush regime can be smaller than that in the vortex liquid regime, because the vortex translational correlation with a length $R_{\rm a}$,[1] which is larger than the Larkin-Ovchinnikov pinning length $R_{\rm c}$,[28] results in the much larger but finite-energy barrier of the vortex motion. The exponential decrease of $\rho(T)$ has been predicted on the basis of the TAFF-type argument in the vortex slush regime,[19] however, $\rho(T)$ in Fig. 3 is well described by the vortex glass theory[24] $\rho\propto(T-T_{\rm g})^s$ and the $T_{\rm g}(H)$ line below the vortex slush regime is continuously connected with that in high fields above $H_{\rm cep}$ as expected in Ref. 27. Since the pinning disorder destroys the long-range translational correlations in high fields above $H_{\rm mcp}$, $R_{\rm a}$ cannot grow to a large size with decreasing temperature and the long-range vortex glass correlation is formed below $T_{\rm g}(H)$. In the vortex slush regime $[T_{\rm g}(H)\leqslant T\leqslant T_{\rm L}(H)]$, the resistivity shows a linear response under low current density which results from the nature of the vortex liquid. However, with increasing current density, vortices with the short-range translational correlations are depinned, so the resistivity shows the nonlinear response. Thus the nonlinear resistivity shown in Fig. 2 is well explained by the vortex dynamics in the vortex slush regime.[19] The results are consistent with our previous report[29] and provide further evidence of the vortex slush regime. The coexistence of the vortex lattice with short-range order and the vortex liquid has been pointed out by the ^{17}O NMR measurements[30] and the result is consistent with our finding in this study. In the vortex slush regime, the total volume with the short-range vortex correlation is estimated to be $\sim 3\%$ as compared with the Bragg glass phase, assuming that the value of Δs reflects the vortex correlation volume. In the weak pinning region between $H^*(T)$ and $T_{\rm m}(H)$ lines, on the other hand, $R_{\rm a}$ becomes larger and the Bragg glass phase with quasi-long-range translational order is stable under the condition of $R_{\rm a}\gg a$.[12–15] Here, a is a vortex lattice spacing.

The appearance of the critical endpoint is supported by recent theories[27,31,32] and Monte Carlo simulations.[33] Since the density is an appropriate order parameter for this kind of transition at $T_{\rm L}(H)$, the two distinct vortex liquid regimes are characterized by the different vortex density reflecting the formation of the short-range translational correlation. Monte Carlo simulations[33] also have shown that the dislocation density of vortices steeply jumps at the transition line between vortex slush and vortex liquid regimes. Although the vortex liquid above $T_{\rm L}(H)$ is denser than the vortex slush below $T_{\rm L}(H)$, two regimes become indistinguishable above $H_{\rm cep}$. These situations are analogous to the first-order liquid-liquid transition line in the pressure-temperature plane for pure substances (e.g., supercooled water,[34] liquid carbon,[35] and liquid phosphorus[36]); in this case, the change in the density results from the different local atomic structures.[34–36] The interesting similarity in the phase diagram between the vortex matter under the controlled disorder (i.e., optimally doped YBCO) and pure substances indicates that the vortex matter behaves as an excellent laboratory for exploring the general phase transition.

C. Vortex phase diagram as a function of the oxygen content

In order to discuss effects of the disorder on the vortex slush regime, let us summarize the vortex phase diagram in YBCO as a function of the oxygen content $y=7-\delta$. The oxygen vacancy δ works as a weak point disorder and the value of y determines the carrier doping level. Figure 6 shows the summary[9,10,16] of the vortex phase diagram of untwinned YBCO as a function of the oxygen content y above and below optimally doping ($y\simeq 6.92$). In the overdoped region ($y>6.92$), the first-order vortex lattice melting transition $T_{\rm m}(H)$ becomes remarkable and the phase transition in the vortex liquid $T_{\rm L}(H)$ is not observed. As shown in Fig. 6(b), slightly overdoped YBCO ($y\simeq 6.95$) shows a typical vortex phase diagram for clean YBCO which has been reported in previous papers.[3,9–11] In the vortex phase diagram, three transition lines $T_{\rm m}(H)$, $T_{\rm g}(H)$, and $H^*(T)$ meet the multicritical point $H_{\rm mcp}$ and divide the vortex state into three different phases, i.e., the vortex liquid, the vortex glass, and the Bragg glass. The topologically ordered Bragg glass phase with quasi-long-range translational order undergoes a transition into the disordered vortex glass phase with increasing field, because the dislocations are induced by the randomly distributed disorder in the high-field region above the field-driven disordering transition line $H^*(T)$; the nature of $H^*(T)$ is well explained by the recent theories.[13–15,27] Since the $H^*(T)$ line and the vortex lattice melting line $T_{\rm m}(H)$ are the boundaries of the Bragg glass phase, both the $H^*(T)$ line and the multicritical point $H_{\rm mcp}$ on the $T_{\rm m}(H)$ line decrease with increasing point disorder in the overdoped region. The precise control of the point disorder in slightly overdoped YBCO ($y\simeq 6.95$) has been performed by the irradiation experiment[10] of 2.5-MeV electrons with a maximum dose of 2×10^{18} $e/{\rm cm}^2$. Although the $T_{\rm c}$ change is 0.4 K after electron irradiation, the value of $H_{\rm mcp}$ reduces from 11 T to 5 T due to the introduced point disorder;[10] the results indicate that the weak point disorder effectively destroys the Bragg glass phase and enhances the vortex glass phase. The thermodynamic evidence of the first-order transition at $H^*(T)$ and the inverse melting of the vortices have been reported in $Bi_2Sr_2CaCu_2O_y$ (Bi2212).[37] The continuous relation between $T_{\rm m}(H)$ and $H^*(T)$ in overdoped YBCO [see Fig. 6(b)] is consistent with the vortex phase diagram in Bi2212.[37]

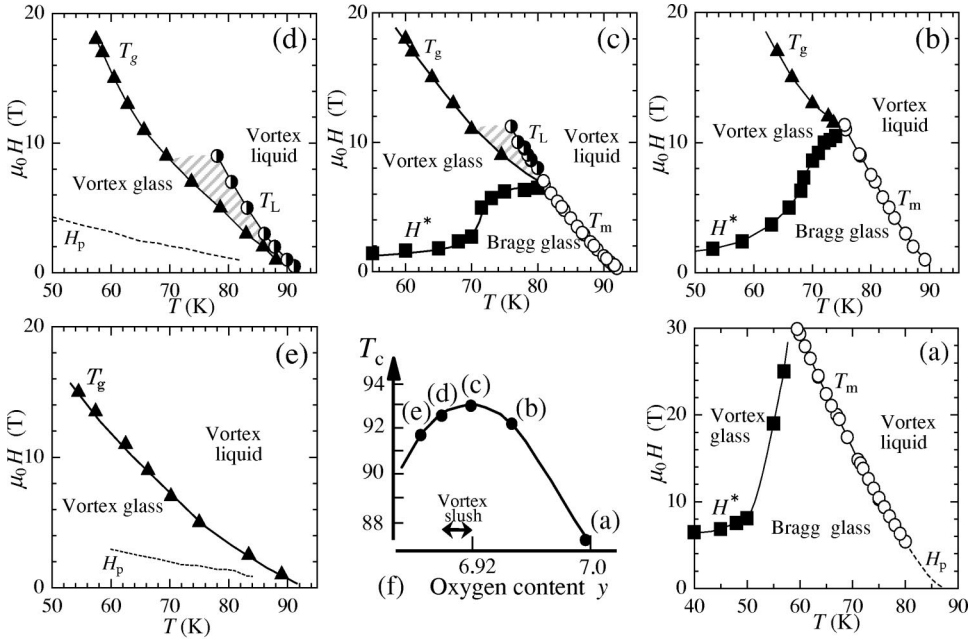

FIG. 6. Vortex phase diagram for untwinned YBCO with various oxygen contents y above and below the optimal condition. (a) Heavily overdoped YBCO ($y \sim 7.0$) (Ref. 16). (b) Slightly overdoped YBCO ($y \simeq 6.95$) (Refs. 9 and 10). (c) Optimally doped YBCO ($y \simeq 6.92$, studied in this paper). (d) Slightly underdoped YBCO ($y \simeq 6.90$) (Ref. 16). (e) Underdoped YBCO ($y \simeq 6.88$). (f) Schematic diagram of T_c vs y. The electron irradiation effect (Ref. 10) has been examined for slightly overdoped YBCO in (b). The shaded portions in (c) and (d) correspond to the vortex slush regime.

In case of heavily overdoped YBCO ($y \sim 7.0$),[16,23] as shown in Fig. 6(a), the first-order melting transition line $T_m(H)$ exists at at least 30 T, which is consistent with the extension of the $T_m(H)$ line of slightly overdoped YBCO. The field-driven disordering transition line $H^*(T)$ shows a large value (~ 6.5 T) even in low temperatures and remarkably increases with increasing temperature above 50 K. Although the vortex glass transition line $T_g(H)$ is not observed in the measured field region, $H^*(T)$ seems to approach the multicritical point H_{mcp} just above 30 T, indicating the similar phase diagram of slightly overdoped YBCO [Fig. 6(b)]. The widely expanded Bragg glass region means that the YBCO single crystals in this study are of intrinsically high quality including a little defect except for the oxygen deficiency. The disappearance of the first-order melting line $T_m(H)$ below the lower critical point $\mu_0 H_{lcp}$ ($\simeq 5$ T) has been studied experimentally[7,23,38] and theoretically.[27] The details of the oxygen content dependence of H_{lcp} will be reported elsewhere.[39]

Since the vortex slush regime is not observed in clean overdoped YBCO but in defect-enhanced YBCO such as proton-irradiated single crystals,[19] thin films,[20] and the single crystal with a low density of twins,[21] the effective disorder plays an important role in the vortex slush regime. In optimally doped YBCO [Fig. 6(c)], the transition line $T_L(H)$ between the vortex liquid and the vortex slush is observed in the limited regions of $\mu_0 H_{mcp}(\simeq 7\ \mathrm{T}) \leqslant \mu_0 H \leqslant \mu_0 H_{cep}$ ($\simeq 11$ T) and 79 K$\leqslant T \leqslant$81 K. With increasing oxygen deficiency from the optimal [Fig. 6(c)] to slightly underdoped [Fig. 6(d)] (Ref. 16) region, the upper limit of the vortex slush (i.e., $\mu_0 H_{cep}$) decreases from 11 T to 9 T. The lower limit of the vortex slush (i.e., $\mu_0 H_{mcp}$) is strongly expanded to lower fields, so the region of the vortex slush becomes wider as shown by the shaded portion in Fig. 6(d); the result well agrees with the phase diagram obtained by ^{17}O NMR measurements.[30] Since the first-order vortex lattice melting transition $T_m(H)$ and the field-driven disordering transition line $H^*(T)$ are not observed in slightly underdoped YBCO ($y \simeq 6.90$), the Bragg glass phase is completely destroyed by the small amount of oxygen deficiency ($\delta \simeq 0.1$).

Figure 6(e) shows the vortex phase diagram for underdoped YBCO ($y \simeq 6.88$). The vortex slush regime disappears and the vortex glass transition is the only visible phase transition; the phase diagram is similar to that of the strongly irradiated YBCO single crystal[25] and disordered YBCO film.[40] The nature of the melting transition was studied by Rykov *et al.*[5] as a function of the oxygen content and the disappearance of the $T_m(T)$ line was observed when the oxygen content decreases below the optimal condition. Our results are consistent with the previous study[5] and provide further information on the vortex solid phase and the vortex slush regime. The vortex liquid-to-slush transition $T_L(H)$ is observable in the narrow region of the field ($H_{mcp} \leqslant H \leqslant H_{cep}$) and the oxygen content ($6.90 \leqslant y \leqslant 6.92$); both H and y are closely related with the disorder strength. The systematic change of the vortex phase diagram in Fig. 6 indicates that the vortex slush regime is located in the borderline below which the vortex lattice melting transition disappears. Therefore, the effective disorder with an intermediate strength, which is controlled by the field and the oxygen content, results in the vortex slush regime between $T_L(H)$ and $T_g(H)$. Recently, the effect of the vortex pinning mechanism on the field-driven disordering transition line $H^*(T)$ was discussed and the vortex phase diagram for two types of pinning (i.e., the δT_c pinning caused by spatial fluctuations of T_c and the δl pinning caused by fluctuations of the charge-carrier mean free path near a lattice defect) has been presented.[32,41] However, the doping dependence of the pinning mechanism has not yet been clear in YBCO. In addition, the pinning mechanism in YBCO is not simple, because the oxygen vacancy forms both clusters along the b axis and the strong atomic distortion along the a axis in the CuO chain layer.[42] The relation between the pinning mechanism and the vortex phase diagram should be studied in future.

In the vortex glass phase in Figs. 6(d) and 6(e), the broad second peak in the magnetization exists and the peak field $H_p(T)$ monotonically decreases toward T_c, contrary to the case of optimally doped and overdoped YBCO. This broad second peak may result from the pinning and dynamics of the collectively pinned disordered vortices.[1] The origin of the broad second peak has been discussed in terms of the field-dependent pinning at oxygen-deficient domains,[43] the crossover in the different regimes of the vortex dynamics,[44] and the collective pinning effects in the disordered vortex phase.[45]

Recently, Bouquet *et al.*[46] also have found the vortex liquid-to-liquid transition from magnetization and specific-heat measurements in YBCO. The reported vortex phase boundary[46] is similar to Fig. 6(c), however, the interpretation is different from that discussed above. Since the specific heat shows the step structure at the liquid-to-liquid transition line which shows no critical endpoint up to 26 T, they have suggested the second-order transition to be from the low-temperature liquid with line tension to the high-temperature liquid without line tension.[47] In addition, Monte Carlo simulations[33,48] using the same three-dimensional frustrated *XY* model show different conclusions each other; Nonomura and Hu[33] have obtained the vortex phase diagram including the vortex slush regime which well agrees with Fig. 6(c), however, Olsson and Teitel[48] have interpreted the line in the liquid phase as a smooth crossover. Further study is required to clarify the details of the vortex phase diagram.

IV. CONCLUSION

We have studied the vortex matter phase diagram for optimally doped untwinned YBCO. We have found that the terminal point of both $T_g(H)$ and $H^*(T)$ lines separates the first-order transition into two lines, i.e., the vortex lattice melting transition line $T_m(H)$ between the vortex liquid and the Bragg glass ($H<H_{mcp}$) and the $T_L(H)$ line, which is characterized by the critical endpoint H_{cep}, between the different kinds of vortex liquid regimes ($H>H_{mcp}$). We have shown that Δs across $T_L(H)$ is much smaller ($\sim 0.02 k_B$/vortex/CuO_2 double layer) than that for the vortex liquid-to-Bragg glass transition at $T_m(H)$. We have presented evidence that, in the vortex slush regime between $T_g(H)$ and $T_L(H)$, the vortices behave as the pinned liquid and the resistivity shows a much smaller but finite value, indicating the short-range translational correlation. We also have studied the vortex phase diagram as a function of y and found that the Bragg glass phase disappears in the underdoped region ($y<6.92$) and the vortex slush regime appears in the narrow region of $6.90 \leqslant y \leqslant 6.92$ due to the intermediate strength of the point disorder.

ACKNOWLEDGMENTS

The authors acknowledge useful discussions with T. Nojima, R. Ikeda, X. Hu, Y. Nonomura, and T. Giamarchi.

*Corresponding author. Electronic address: terukazu@imr.edu

[1] G. Blatter, M.V. Feigel'man, V.B. Geshkenbein, A.I. Larkin, and V.M. Vinokur, Rev. Mod. Phys. **66**, 1125 (1994).

[2] H. Safar, P.L. Gammel, D.A. Huse, D.J. Bishop, J.R. Rice, and D.M. Ginsberg, Phys. Rev. Lett. **69**, 824 (1992); W.K. Kwok, S. Fleshler, U. Welp, V.M. Vinokur, J. Downey, and G.W. Crabtree, *ibid.* **69**, 3370 (1992); *ibid.* **72**, 1092 (1994).

[3] H. Safar, P.L. Gammel, D.A. Huse, D.J. Bishop, W.C. Lee, J. Giapintzakis, and D.M. Ginsberg, Phys. Rev. Lett. **70**, 3800 (1993).

[4] U. Welp, J.A. Fendrich, W.K. Kwok, G.W. Crabtree, and B.W. Veal, Phys. Rev. Lett. **76**, 4809 (1996); Ruixing Liang, D.A. Bonn, and W.N. Hardy, *ibid.* **76**, 835 (1996); T. Nishizaki, Y. Onodera, T. Naito, and N. Kobayashi, J. Low Temp. Phys. **105**, 1183 (1996).

[5] A.I. Rykov, S. Tajima, F.V. Kusmartsev, E.M. Forgan, and Ch. Simon, Phys. Rev. B **60**, 7601 (1999).

[6] A. Schilling, R.A. Fisher, N.E. Phillips, U. Welp, D. Dasgupta, W.K. Kwok, and G.W. Crabtree, Nature (London) **382**, 791 (1996).

[7] A. Junod, M. Roulin, J.Y. Genoud, B. Revaz, A. Erb, and E. Walker, Physica C **275**, 245 (1997); M. Roulin, A. Junod, A. Erb, and E. Walker, Phys. Rev. Lett. **80**, 1722 (1998).

[8] X. Hu, S. Miyashita, and M. Tachiki, Phys. Rev. Lett. **79**, 3498 (1997).

[9] T. Nishizaki, T. Naito, and N. Kobayshi, Phys. Rev. B **58**, 11169 (1998).

[10] T. Nishizaki, T. Naito, S. Okayasu, A. Iwase, and N. Kobayashi, Phys. Rev. B **61**, 3649 (2000).

[11] K. Deligiannis, P.A.J. de Groot, M. Oussena, S. Pinfold, R. Langan, R. Gagnon, and L. Taillefer, Phys. Rev. Lett. **79**, 2121 (1997); H. Küpfer, Th. Wolf, C. Lessing, A.A. Zhukov, X. Lancon, R. Meier-Hirmer, W. Schauer, and H. Wuhl, Phys. Rev. B **58**, 2886 (1998); D. Giller, A. Shaulov, Y. Yeshurun, and J. Giapintzakis, *ibid.* **60**, 106 (1999); S. Kokkaliaris, P.A.J. de Groot, S.N. Gordeev, A.A. Zhukov, R. Gagnon, and L. Taillefer, Phys. Rev. Lett. **82**, 5116 (1999).

[12] T. Giamarchi, and P.L. Doussal, Phys. Rev. Lett. **72**, 1530 (1994); Phys. Rev. B **52**, 1242 (1995); **55**, 6577 (1997).

[13] D. Ertas and D.R. Nelson, Physica C **272**, 79 (1996).

[14] J. Kierfeld, Physica C **300**, 171 (1998).

[15] D. Carpentier, P.L. Doussal, and T. Giamarchi, Europhys. Lett. **35**, 379 (1996); J. Kierfeld, T. Nattermann, and T. Hwa, Phys. Rev. B **55**, 626 (1997); D.S. Fisher, Phys. Rev. Lett. **78**, 1964 (1997); V. Vinokur, B. Khaykovich, E. Zeldov, M. Konczykowski, R.A. Doyle, and P.H. Kes, Physica C **295**, 209 (1998).

[16] T. Nishizaki, K. Shibata, T. Naito, M. Maki, and N. Kobayashi, J. Low Temp. Phys. **117**, 1375 (1999).

[17] K. Shibata, T. Nishizaki, T. Sasaki, and N. Kobayashi, Physica B **294-295**, 354 (2001).

[18] W.K. Kwok (unpublished).

[19] T.K. Worthington, M.P.A. Fisher, D.A. Huse, J. Toner, A.D. Marwick, T. Zabel, C.A. Field, and F. Holtzberg, Phys. Rev. B **46**, 11 854 (1992).

[20] H.H. Wen, S.L. Li, G.H. Chen, and X.S. Ling, Phys. Rev. B **64**, 054507 (2001).

[21] D. Pal, S. Ramakrishnan, A.K. Grover, D. Dasgupta, and K.

Sarma, Phys. Rev. B **63**, 132505 (2001); L. Miu, *ibid.* **65**, 096501 (2002); D. Pal, S. Ramakrishnan, and A.K. Grover, *ibid.* **65**, 096502 (2002).

[22] D.J.L. Hong and D.M. Smith, J. Am. Chem. Soc. **74**, 1751 (1991); R. Liang, D.A. Bonn, and W.N. Hardy, Physica C **304**, 105 (1998); S. Kokkaliaris, A.A. Zhukoov, P.A.J. de Groot, R. Gagnon, L. Taillefer, and T. Wolf, Phys. Rev. B **61**, 3655 (2000).

[23] T. Nishizaki, K. Shibata, T. Sasaki, and N. Kobayashi, Physica C **341-348**, 957 (2000).

[24] M.P.A. Fisher, Phys. Rev. Lett. **62**, 1415 (1989); D.S. Fisher, M.P.A. Fisher, and D.A. Huse, Phys. Rev. B **43**, 130 (1991).

[25] A.M. Petrean, L.M. Paulius, W.K. Kwok, J.A. Fendrich, and G.W. Crabtree, Phys. Rev. Lett. **84**, 5852 (2000).

[26] V.M. Vinokur, M.V. Feigel'man, V.B. Geshkenbein, and A.I. Larkin, Phys. Rev. Lett. **65**, 259 (1990).

[27] R. Ikeda, J. Phys. Soc. Jpn. **65**, 3998 (1996); *ibid.* **70**, 219 (2001).

[28] A.I. Larkin and Y.N. Ovchinnikov, J. Low Temp. Phys. **34**, 409 (1979).

[29] N. Kobayashi, T. Nishizaki, K. Shibata, T. Sato, M. Maki, and T. Sasaki, Physica C **362**, 121 (2001).

[30] A.P. Reyes, X.P. Tang, H.N. Bachman, W.P. Halperin, J.A. Martindale, and P.C. Hammel, Phys. Rev. B **55**, R14737 (1997); H.N. Bachman, A.P. Reyes, V.F. Mitrovic, W.P. Halperin, K. Kleinhammes, P. Kuhns, and W.G. Moulton, Phys. Rev. Lett. **80**, 1726 (1998).

[31] J. Kierfeld, and V. Vinokur, Phys. Rev. B **61**, R14928 (2000).

[32] G.P. Mikitik and E.H. Brandt, Phys. Rev. B **64**, 184514 (2001); E. H. Brandt and G. P. Mikitik, Physica C (to be published).

[33] Y. Nonomura, and X. Hu, Phys. Rev. Lett. **86**, 5140 (2001).

[34] O. Mishima, and H.E. Stanley, Nature (London) **396**, 329 (1998); K. Koga, H. Tanaka, and X.C. Zeng, *ibid.* **408**, 564 (2000).

[35] J.N. Glosli, and F.H. Ree, Phys. Rev. Lett. **82**, 4659 (1999).

[36] Y. Katayama, T. Mizutani, W. Utsumi, O. Shimomura, M. Yamakata, and K. Funakoshi, Nature (London) **403**, 170 (2000); G. Franzese, G. Malescio, A. Skibinsky, S.V. Buldyrev, and H.E. Stanley, *ibid.* **409**, 692 (2001).

[37] N. Avraham, B. Khaykovich, Y. Myasoedov, M. Rappaport, H. Shtrikman, D.E. Feldman, T. Tamegai, P.H. Kes, M. Li, M. Konczykowski, K. van der Beek, and E. Zeldov, Nature (London) **411**, 451 (2001).

[38] A.A. Zhukov, P.A.J. de Groot, S. Kokkaliaris, E. di Nicolo, A.G.M. Jansen, E. Mossang, G. Martines, P. Wyder, T. Wolf, H. Küpfer, H. Asaoka, R. Gagnon, and L. Taillefer, Phys. Rev. Lett. **87**, 017006 (2001).

[39] T. Nishizaki, K. Shibata, and N. Kobayashi (unpublished).

[40] R.H. Koch, V. Foglietti, W.J. Gallagher, G. Koren, A. Gupta, and M.P.A. Fisher, Phys. Rev. Lett. **63**, 1511 (1989).

[41] Y. Radzyner, A. Shaulov, and Y. Yeshurun, Phys. Rev. B **65**, 100513 (2002).

[42] T. Nishizaki, K. Shibata, M. Maki, and N. Kobayashi, J. Low Temp. Phys. (to be published); M. Maki, T. Nishizaki, K. Shibata, and N. Kobayashi, J. Phys. Soc. Jpn. **70**, 1877 (2001).

[43] M. Daeumling, J.M. Seuntjens, and D.C. Larbalestier, Nature (London) **346**, 332 (1990); J.L. Vargas, and D.C. Larbalestier, Appl. Phys. Lett. **60**, 1714 (1992).

[44] L. Krusin-Elbaum, L. Civale, V.M. Vinokur, and F. Holtzberg, Phys. Rev. Lett. **69**, 2280 (1992); Y. Abulafia, A. Shaulov, Y. Wolfus, R. Prozorov, L. Burlachkov, Y. Yeshurun, D. Majer, E. Zeldov, H. Wühl, V.B. Geshkenbein, and V.M. Vinokur, *ibid.* **77**, 1596 (1996).

[45] T. Nishizaki, T. Naito, and N. Kobayashi, Physica C **317-318**, 645 (1999).

[46] F. Bouquet, C. Marcenat, E. Steep, R. Calemczuk, W.K. Kwok, U. Uelp, G.W. Crabtree, R.A. Fisher, N.E. Phillips, and A. Schilling, Nature (London) **411**, 448 (2001).

[47] Z. Tešanović, Phys. Rev. B **51**, 16 204 (1995); **59**, 6449 (1999); A.K. Nguyen and A. Sudbø, *ibid.* **60**, 15 307 (1999).

[48] P. Olsson and S. Teitel, Phys. Rev. Lett. **87**, 137001 (2001).